

RSC Advances

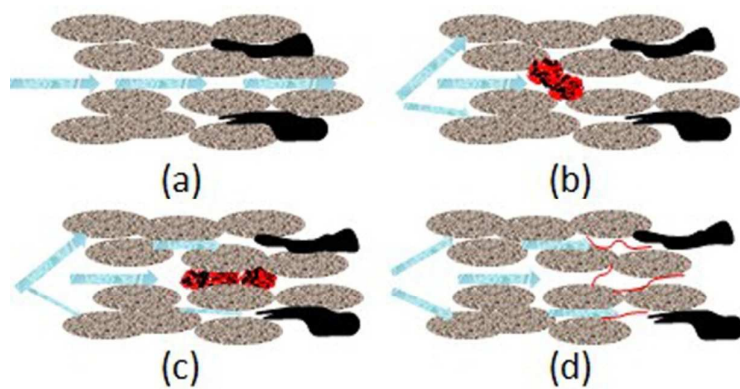


This is an *Accepted Manuscript*, which has been through the Royal Society of Chemistry peer review process and has been accepted for publication.

Accepted Manuscripts are published online shortly after acceptance, before technical editing, formatting and proof reading. Using this free service, authors can make their results available to the community, in citable form, before we publish the edited article. This *Accepted Manuscript* will be replaced by the edited, formatted and paginated article as soon as this is available.

You can find more information about *Accepted Manuscripts* in the [Information for Authors](#).

Please note that technical editing may introduce minor changes to the text and/or graphics, which may alter content. The journal's standard [Terms & Conditions](#) and the [Ethical guidelines](#) still apply. In no event shall the Royal Society of Chemistry be held responsible for any errors or omissions in this *Accepted Manuscript* or any consequences arising from the use of any information it contains.



DCPM is served as conformance control agents and polymer flooding within deep formation

Degradable cross-linked polymeric microsphere for enhanced oil recovery applications

Xiaorong Yu*^a, Wanfen Pu^b, Dajun Chen^a, Jian Zhang^a, Fei Zhou^c, Rui Zhang^a

Gu Siman^d

^a School of Chemistry and Chemical Engineering, Southwest Petroleum University, 610500, Chengdu, People's Republic of China. E-mail: 619471801@qq.com

^b School of Oil & Natural Gas Engineering, Southwest Petroleum University, Chengdu, People's Republic of China

^c Drilling & Production Technology Research Institute of CNPC Liaohe Oilfield, Pan jin, People's Republic of China

^d State Key Laboratory of Oil and Gas Geology and Exploitation, South West Petroleum University, Chengdu, People's Republic of China

Abstract

In this paper, a degradable cross-linked polymeric microsphere (DCPM) was prepared by inverse emulsion polymerization using acrylamide (AM), 2-methyl-2-acrylic amide propyl sulfonic acid (AMPS) and alpha methyl styrene (HM) as monomers, using polyethylene glycol(200) diacrylate (PEG-200 diacrylate) as labile crosslinkers. The optimized synthesis conditions of DCPM were also investigated. DCPM was characterized by Infrared spectroscopy, ¹H-NMR, laser particle analyzer and elemental analysis. Mechanical stability experiments showed that DCPM processed superior anti-shear properties compared with DPM without PEG-200 diacrylate. SEM and viscosity experiments demonstrated that the degradation process of DCPM might be described from initially absorbing amount of water to swell to finally degrading into linear polymer. In addition, the effects of salinity, temperature, PEG-200 diacrylate content and DCPM content on the degradation performance of DCPM dispersed in aqueous solutions were also studied. Finally, sandpacks flooding experiments showed that DCPM initially served as a conformance control agent to plug high thief zones and subsequently acted as polymer for oil displacement within

the deep reservoir to enhance oil recovery.

Keywords

Enhanced oil recovery; Deep conformance control; Inverse emulsion polymerization; Degradable cross-linked polymeric microsphere

1. Introduction

Excessive water production from hydrocarbon reservoirs is one of the most serious problem in the mature oil field by prolonged water flooding development, which brings many problems such as additional lifting, separating and treatment costs, as well as environmental problems associated with brine disposal and rapid productivity decline.¹⁻²

Over the years, methods for treating the unwanted water were referred to as conformance control, mainly including polymers and polymer derived gels. However, conventional techniques for conformance control have found to be restricted in the near well-bore regions due to the high viscosity of polymers and the fast gelling rate of polymer gels.³⁻⁴ Moreover, These near well-bore treatments become ineffective when high permeability thief zones are in hydraulic contact with lower permeability zones with high remaining oil saturation. In such cases, an in-depth conformance strategy appears to be more effective by redistricting the injection water in the reservoir and mobilizing the remaining oil.⁵

Presently, the cross-linked polymer microspheres served to provide in-depth conformance control have attracted more attentions because of many merits such as size-controlled, highly swelling, tolerant to temperature and salinity and environmentally friendly.⁶⁻⁷ However, N-methylene bisacrylamide (NMBA) was used as crosslinkers in conventional polymer microspheres, which led to microspheres just swell but do not dissolve in contact with water, resulting in poor mobility control within deep formation. ⁸⁻⁹ In 1999, The Bright Water microspheres in which the conformation was constrained by two types of crosslinkers, was introduced. While they were partial dissolved in hot water. These microspheres now available at industrial scale, have been shown to have attractive properties for water shut off and conformance control operations, but the decomposition of labile crosslinkers was ill

described. 10-13 Lately, Paul presented a degradable nanocomposite performed particle gel, whereas they concentrated on the improvement in nanocomposite gel properties and behavior by the addition of nanocomposite compared with conventional hydrogels without any nanomaterial, while the degradation of nanocomposite gel was barely studied. 14

Thus, inspired by the methods of labile crosslink of Bright Water microspheres, we prepared a degradable cross-linked polymeric microsphere, called DCPM, which only involved labile crosslinks in it. The incorporation of labile crosslinkers not only imparts excellent performance of conventional polymeric microspheres such as swelling ability, mechanical stability and plugging ability to DCPM, but results in improvement in post-degradation solution viscosity after the DCPM degrades under reservoir conditions. The novelty of this work involves a dramatic increase in post-degradation solution viscosity compared to currently existing microspheres, which endows DCPM with the dual properties of conformance control and polymer flooding within deep formation. The schematic diagram of DCPM for conformance control and polymer flooding within deep formation is presented in Fig.1(see in supplementary information).

As shown in Fig. 1, (a)Before treating, the injected water follows the path of high permeability zones, bypassing large amount of oil in low permeability zones which resulting in the poor recovery. (b)DCPM, when dispersed the into injected water, the particles can propagate through matrix rock until the temperature rises. And then they absorb the surrounding water to swell , form associations ,and act as conformance control agents by plugging water-thief zones and channels, thereby directing chase water to displace un-swept oil from low permeability oil-rich zones.(c) DCPM will be deformed through the pore throat to plug the next pore throat within the deep reservoir to achieve the conformance control step-by-step. (d)After an extended time period, DCPM degrades into a highly viscous polymer solution that moves deeper into the reservoir, and then mixes with flood water and increases its viscosity to achieve polymer flooding for improving oil recovery .Therefore, the viscosity of DCPM is of key concern after it degrades.

The purpose of this paper include the following sections.(1) DCPM was prepared by inverse emulsion polymerization and the optimized copolymerization conditions were investigated.(2) The basic performances of DCPM such as chemical structure , element composition, particle size distribution and mechanical stability were characterized.(3)The degradation performances of DCPM and their influence factors were investigated by SEM and viscosity measurement experiments.(4) Sandpacks flooding experiments were conducted to evaluate the oil displacement property of DCPM.

2. Experimental

2.1. Materials

The materials were used in experiments without further purification, including monomer acrylamide(AM), 2-acrylamide-2-methyl propanesulfonic acid (AMPS), alpha methyl styrene(HM), 2'-azobis(2-amidinopropane) dihydrochloride(V-50, initiator), polyoxyethylene(80) sorbian monooleate(T-80, nonionic surfactant), sorbitan monooleate(S-80, nonionic surfactant), polyethylene glycol(200) diacrylate (PEG-200 diacrylate, labile crosslinkers), sodium chloride(NaCl), anhydrous calcium chloride (CaCl₂), magnesium chloride(MgCl₂), anhydrous ethanol. All of the above reagents were purchased from Kelong, Chengdu, China. Deionized water and fresh water were obtained in own laboratory. Crude oil of Changqing oilfield was provided by Research institute of Changqing.

2.2. Synthesis of DCPM

DCPM was prepared by polymerizing a monomer emulsion consisting of an aqueous mixtures of AM(20 g) , AMPS(5 g), NaOH(0.96 g) and deionized water(25 g) as the dispersed phase and a mixture of HM(0.1 g), PEG-200 diacrylate(0.25 g), S-80(7.02 g),T-80(0.98 g) and white oil (40 g) as the continuous phase. The monomer emulsion was obtained by mixing the aqueous phase and the oil phase in a three-neck round-bottom flask equipped with a mechanical stirrer by 800 rpm at 30 °C for 30 minutes. After deoxygenation with nitrogen for 1 hour, polymerization was initiated by using 50 mg of V-50 at 50 °C under stirring of 300 rpm. After the temperature peaks, the reaction lasted for an additional 4 hours to form the product. If desired,

DCPM can be isolated from the latex by precipitating, filtering, and washing with ethanol for several times to remove the remaining monomer, white oil and surfactant. Thereafter, DCPM was oven-dried at 45 °C for 48 hours for further characterization and analysis.

For DPM, the same procedure was followed except that PEG-200 diacrylate was excluded. For DCPM with different amounts of PEG-200 diacrylate, the same procedure was followed and just varied the dosage of PEG-200 diacrylate.

2.3. Characterization

2.3.1. Fourier transform infrared (FTIR) and NMR analysis

The FTIR spectrum was obtained with a Perkin Elmer RX-1 spectrophotometer (Beijing Reili Analytical Instrument) in the optical range of 400-4000 cm^{-1} and its resolution was 4 cm^{-1} and the scanning number was 32. The KBr pellets were prepared with the purified DCPM sample.

The purified DCPM was dissolved in D_2O and the measurement was conducted at room temperature by a 400-MHz BRUKER FT-NMR spectrometer (Bruker Company, Switzerland).

2.3.2. Scanning Electron Microscope(SEM)analysis

The surface morphology of DCPM was examined by a Quanta 450 scanning electron microscope(SEM) instrument(Fez Co). Dried and purified samples were first frozen overnight and then lyophilized, sputter-coated with gold in an inert argon atmosphere.

2.3.3. Particle size determination

Malvern laser particle size analyzer (HYDRO2000(APA2000), Malvern ,UK)was used to determine the particle size of DCPM. The prepared DCPM were diluted with saline water composed of 5000 mg/L NaCl to control the swelling of DCPM .

2.3.4. Elementary Analysis of DCPM

The elemental analysis of DCPM was conducted by Vario EL-III elemental analyzer (Elementar, German) to determine the content of carbon, nitrogen, hydrogen and sulfur.

2.3.5. Conversion determination

The conversion of AM was determined by high performance liquid chromatography technology (Shimadzu company, Japan). The conversion of AM was calculated with

the following equation.15

$$C\% = \frac{W_{AM} - \frac{AC_0}{A_0} \times V}{W_{AM}} \times 100\% \quad (1)$$

Here, C is the conversion of AM, W_{AM} is the total weight of AM in the reaction, C_0 is the concentration of standard sample of AM, A_0 is the chromatographic peak area of standard sample of AM, A is the chromatographic peak area of the un-reacted AM, and V is the solution volume of ethanol in which DCPM was isolated by precipitation.

2.3.6. Solution viscosity measurement

The viscosity of DCPM aqueous dispersions was measured at the shear rate of 7.34 sec^{-1} using a Brookfield DV-III viscometer with a NO.0 spindle at 25 °C .

2.3.7. Sandpacks flooding experiments

Sandpacks flooding experiments were conducted to evaluate the performance of DCPM in enhanced oil recovery. The materials employed in this section included crude oil of Changqing with a viscosity of 15 mPa·s at 90 °C and formation water of Changqing(30000 mg/LNaCl+100mg/LCaCl₂+30mg/LMgCl₂). The DCPM dispersed in formation water was fixed at 300 mg/L. Sandpacks prepared by beach sand (60~150 mesh) were used to simulate the porous media. The basic parameters of sandpacks are listed in Table 1(see in supplementary information).The steps for flooding experiments were described below.

(1) Sandpacks were saturated separately with formation water to calculate water permeability (K_{rw})on basis of Darcy's law.

(2) Crude oil of Changqing was injected into the sandpacks until formation water ceased, and then the oil saturation (S_o)was obtained.

(3) Injecting the formation water until a water cut of 95% were gained. Then, the DCPM dispersed in the formation water(300 mg/L) was injected for 0.5PV.

Subsequently, the core flow testing apparatus was shut in to allow the DCPM to degrade into linear polymers at 90°C for 10 days. At last, only formation water was injected until an extreme water cut of 98% were reached.

Meanwhile, the injection pressure was recorded and the effluent oil was collected for calculating the recovery. The injection rate of crude oil, formation water and DCPM

dispersions was 2 mL/min. The experimental temperature was at 90 °C.

3. Results and Discussion

3.1. IR Spectra and ¹H-NMR Analysis

The chemical structures of PAM and DCPM were analyzed by FT-IR (Fig. 2). From the spectra, two strong absorption peaks at 3444 and 1660 cm⁻¹ signify the stretching vibration of N-H and C=O respectively in AM, and the absorption peaks at 2727 and 2840 cm⁻¹ refer to the stretching vibration of CH₃ and CH₂ respectively. These results demonstrate the presence of typical structure of AM in the target samples. Compared with spectra A, absorption band at 3037 cm⁻¹ in spectra B attributes to the framework vibration of arene, and absorption peaks at 1600 and 1500 cm⁻¹ are due to C=C of aromatic ring. Additionally, the fingerprints bands from 650-800 cm⁻¹ confirm that alpha-methyl styrene was successfully incorporated into the copolymer chain. The sharp and strong absorption peak at 1037 cm⁻¹ is assigned to the asymmetric stretching vibration of S=O. In conclusion, all these characteristic peaks confirm that DCPM is the copolymerized product of AM, AMPS and HM.

The product was further characterized by NMR spectra (Fig. 3, see in supplementary information). Fig. 3 presents the ¹H NMR spectrum of DCPM in D₂O. All the resonances of protons are as follows: 6H (—CH₃ of AMPS side chain), δ 1.659 ppm; 2H (—CH₂ of AMPS side chain), δ 3.392 ppm; 2H (—CH₂ of AMPS main chain), δ 1.762 ppm; 1H (—CH of AMPS main chain), δ 2.35-2.42 ppm; 2H (—CH₂ of AM main chain), δ 1.432 ppm; 1H (—CH of AM main chain), δ 2.65 ppm; 4H (—CH of phenyl), δ 7.29~7.76 ppm; 1H (—CH of HM main chain), δ 2.67~2.83 ppm; 2H (—CH₂ of HM main chain), δ 2.115~2.23 ppm; 3H (—CH₃ of HM side chain), δ 1.25~1.32 ppm; 1H (—CH of PEG-200 diacrylate main chain), δ 1.07 ppm; 2H (—CH₂ of PEG-200 diacrylate main chain), δ 2.44 ppm; peaks at 3.73~4.18 ppm attributed to the protons of —OCH₂CH₂O— in PEG-200 diacrylate. The results showed that the synthesized product was the terpolymer of AM, AMPS, HM and PEG-200 diacrylate.

3.2. Elementary Analysis of DCPM

The molar composition of monomer feed and DCPM are listed in Table 2. It can be

found that the molar composition of DCPM is close to the monomer feed composition, which indicated that the copolymerization of DCPM occurred according to the theoretical design.

3.3. Particle size analysis

The particle size distribution of DCPM was estimated by laser particle size analyzer (Fig. 4), which indicates that DCPM suspensions possess a narrow size distribution and the average particle size is 25.6 μm . In addition, SEM results show that DCPM is spherical and monodisperse with a size of 5 μm . Obviously, diameters of DCPM obtained by SEM are smaller than those obtained from laser particle size analyzer. The probable reason for this discrepancy can be found in the different sample preparation according to disparate measurement method.¹⁶ For laser particle size analyzer, the measurements were made in a highly diluted suspension, where the DCPM was in swollen state and expand several times of its original size. Nevertheless, the SEM studies were based on dried samples and the molecule chain of the DCPM was in a finite state, which thus led to a decrease in size by contrast with the data obtained from laser particle size analyzer.

3.4. Mechanical stability

Mechanical stability of DCPM and DPM without PEG-200 diacrylate were carried out by measuring apparent viscosity before and after applications of high shear rate at 3000 rpm for 5 minutes. As shown in Fig. 5, the apparent viscosity of DCPM seems to be unchanged and as near as possible to that of water before and after high shearing. However, the apparent viscosity of DPM decreases dramatically from 69.3 mPa·s to less than 10 mPa·s under the same condition. This might be ascribed to the breakage of the polymer backbone of DPM resulting in an irreversible decrease in viscosity of DPM.¹⁷ Nevertheless, the polymer chains of DCPM are constrained by internal crosslinking of PEG-200 diacrylate, which endows the rigidity of DCPM leading to a good mechanical stability of DCPM.

3.5. Optimization of the Reaction Conditions

Previous studies had shown that an effective block could be achieved unless the particle size of DCPM matched with that of pore throat (sub-micron or micron).¹⁸ In

this study, the particle size and conversion rate of DCPM were taken as indexes to optimize the synthetic conditions. The basic recipe for the preparation of DCPM was listed in Table 3(see in supplementary information).

3.5.1 The effect of monomer concentration

The effect of monomer concentration on the particle size and conversion of DCPM was investigated with other conditions unchanged(Table 3), the results are exhibited in Fig. 6 (see in supplementary information). As shown in Fig. 6, the median size of DCPM increased with the addition of monomer concentration, while the conversion decreased when the monomer concentration was at 35% and the reaction system was unstable. The 25% of monomer concentration was effective to obtain the DCPM with the median size of 30.2 μm and the conversion of more than 85%.

3.5.2 The effect of monomer ratio

Fig. 7(see in supplementary information) shows the influence of monomer ratio on the particle size and conversion of DCPM holding other conditions constant (Table 3).It was found that the particle size of DCPM increased with the addition of HM. This might be due to the hydrophobicity of HM, which resulted in the association of DCPM to form the larger particles. The decrease of conversion could be understood by the space-steric effect of AMPS and the low free radicals activity of HM. Therefore, the promising monomer ratio of AM,AMPS and HM was 20:5:0.2.

3.5.3 The effect of volume ratio of oil-water

The results of median size and conversion of DCPM are presented in Fig. 8(see in supplementary information) by varying the volume ratio of oil- water and keeping other factors unchanged (Table 3).

It was found that (Fig. 8) both the particle size and conversion of DCPM decreased with the increase of the volume ratio of oil-water. This could be responsible for that monomer aqueous solution was dispersed into smaller droplets in the oil phase with the aid of emulsifier by increasing the volume fraction of oil ,meanwhile the oil phase could scatter the polymerization heat and prevent the monomer droplet from aggregating, which brought about the smaller particle size. The decrease of conversion could be due to the chain transfer effect. Therefore, comprehensively considering the particle size and conversion, the advisable volume ratio of oil-water was 5:4.

3.5.4 The effect of emulsifier concentration

As shown in Fig. 9 (see in supplementary information), both the conversion and particle size of DCPM decreased with the increase of emulsifier concentration. These appearances could be understood as below. The addition of emulsifier was conducive to the dispersion of monomer aqueous solutions into small droplets, and emulsifiers could absorb on the surface of monomer droplets hindering the coalescence of droplets and stabilizing the reaction system, which led to the smaller particle size. While the decrease of conversion might be ascribed to the effect of chain transfer and the low initiation efficiency. Thus, the befitting concentration of emulsifiers should be of 7%.

3.5.5 The effect of initiator

Three kinds of initiators with various concentrations were studied, the results are listed in Table 4 (see in supplementary information). It can be observed that the reaction rate of AIBN is too fast to control, and that of $K_2SO_4/NaHSO_3$ is too slow, which results in an unstable reaction system or the low conversion (less than 20%). While, the uniform products with moderate reaction rate and high conversion more than 80% can be obtained by the addition of V-50 at 0.4 - 0.6%.

3.6. Degradable performance experiments of DCPM

3.6.1 Degradable process of DCPM

Degradable process of DCPM tests were separately conducted by viscosity measurements and SEM.

Aqueous suspensions of DCPM (0.3 wt%) were prepared by fresh water and the aging temperature was at 90 °C, the viscosity of DCPM suspensions was measured at different aging days. The results are presented in Table 5. As listed in Table 5, the viscosity of DCPM suspensions first increased with the prolonging of aging time and then remained constant with the time. This might be ascribed to the thermal degradation of PEG-200 diacrylate, releasing a low molecular weight linear polymer, increasing the polymer solution viscosity.

To confirm these results, aqueous suspensions of DCPM (0.3 wt%) prepared by fresh water were aged at 90 °C for different days. After the specified aging times, a sample was taken out of the oven and cooled to room temperature, following by the sample preparation of freezing and lyophilizing. SEM was conducted to help us understand

the degradation nature of DCPM.

As presented in Fig.10. It can be observed that DCPM mainly expands in fresh water after the aging time of 1 day (b) and the particle diameter is about three times the size of the original one (a), and also maintain the anomalous spherical structure. Whereas at the aging time of 3 days (c), the spherical structures decrease dramatically and DCPM particles aggregate with each other. In 7 days, the spherical structure is almost disappeared (d) and amounts of linear structures can be found at 10 days (e), signifying the degradation of the crosslinked microspheres. Worthy of mention is that similar linear structures can be observed in both DCPM after degradation (e) and DPM without crosslinking (f), indicating that the degradation of crosslinked microspheres into polymer solutions. This, we ascribe to the thermal degradation of PEG-200 diacrylate. In conclusion, the degradation process of DCPM might be described from initially absorbing amount of water to swell to finally degrading into linear polymer.

3.6.2 Degradable performance of DCPM in aqueous dispersions

As discussed that DCPM could degrade into polymers to make the water viscous. While the degradable performance of DCPM could be affected by various factors due to the complex chemical surrounding environment of the reservoir. Therefore, more detailed information about the viscosities of degradable performance of DCPM in aqueous dispersions is discussed in the following sections.

(1) Salinity

In this study, DCPM was used at a given content of 0.3 wt% at 90°C, while its salt solutions were prepared separately with NaCl, CaCl₂, and MgCl₂ (0 mg/L, 10000 mg/L Na⁺, 10000 mg/L Na⁺+100 mg/L Ca²⁺, 10000 mg/L Na⁺+100 mg/L Ca²⁺+100 mg/L Mg²⁺, 50000 mg/L Na⁺+100 mg/L Ca²⁺+100 mg/L Mg²⁺).

As presented in Fig. 11, the viscosities of DCPM increase with the time and reach to the maximum value at 7 days in regardless of fresh water or saline water, and then remain unchanged with the prolonging of aging time. However, the viscosities of DCPM decrease with the addition of salt, especially for that of 50000 mg/L Na⁺. The reasons might be that the shielding effects of metal ions weaken the electrostatic repulsion between the molecular chain, and lead to the shrinkage of polymer chains,

which results in an decrease in viscosity.²⁰⁻²¹ More interesting, it can be found that the viscosity of DCPM with 10000 mg/L Na⁺+100mg/L Ca²⁺ is a slight higher than that with 10000 mg/L Na⁺. The possible reason is that Ca²⁺ crosslinked with COO⁻ of degradable DCPM to form intermolecular crosslinking which increase the final viscosity.²³

(2) Temperature

In this section, DCPM dispersions were prepared by fresh water with the concentration of 0.3 wt%, the aging temperature varied from 70 to 120 °C. As shown in Fig. 12, It can be found that there are great differences between viscosities of DCPM at different temperature. For 70 °C, viscosity of DCPM increases with the time, that at 90 °C first increases in 10 days and then remains unchanged. While viscosity of DCPM first increases and then decreases when the aging temperature is higher than 100 °C. The probable reasons can be interpreted as follows, on the one hand, the degradation rate of PEG-200 diacrylate increases with an increase of temperature which contributes to the formation of more and more linear polymer and thus leads to a high viscosity. On the other hand, an increase of temperature intensifies the molecular movement resulting in the destruction of hydration film of polymer and bringing about a reduction in viscosity. The above two opposite effects exist together and determine the final viscosity of DCPM dispersions. As for the low temperature of 70 °C, the decomposition of PEG-200 diacrylate contributes more to the viscosity of DCPM dispersions. In addition, introduction of the temperature tolerance monomers such as AMPS and HM into the copolymer also have positive effect on the viscosity of DCPM dispersions, all these effects cause the increasing viscosity of DCPM dispersions with the extension of aging time at 70 °C. As for 90 °C, it is clearly that the decomposition of PEG-200 diacrylate advantages in 10 days, but later the temperature begins to have an adverse effect on viscosity. However, an increase of viscosity resulted from the decomposition of PEG-200 diacrylate is enough to offset the reduction of viscosity caused by the high temperature, and thus the viscosity remains constant. When the aging temperature is higher than 100 °C, a significant increase of viscosity is mainly ascribe to the degradation of PEG-200 diacrylate in

the first days, But later the high temperature has predominance in viscosity, and finally leads to a reduction of viscosity.

(3) PEG-200 diacrylate content

DCPM fresh water dispersions were used at a constant concentration of 0.3 wt%, the aging temperature was at 90 °C. DCPM were prepared by adding varied contents(1.6~5 wt%) of PEG-200 diacrylate. As presented in Fig. 13. It can be found that the more the PEG-200 diacrylate, the lower the initial viscosity. Tiny changes of viscosity could be observed in the aging time of 20 days for the content of PEG-200 diacrylate at 5 wt%. A reasonable explanation might be that the crosslink density is high enough to form denser 3-D network structure, which reduces the swelling capability of DCPM, and most of low molecular polymers are confined to form little liner polymer, and thus the viscosity is very low. As for PEG-200 diacrylate with a low content at 1.6 wt%, it can be noted that the viscosity rises sharply to the maximum value of 96 mPa·s in 4 days .This is because the lower the PEG-200 diacrylate, the sparser the crosslink density. Which leads to the formation of more and more linear polymer resulting in a high viscosity. However, the reduction of the viscosity at 8 days is mainly due to the thermal degradation of polymer at high temperature.

(4) DCPM content

DCPM aqueous dispersions were prepared by fresh water, the aging temperature was at 90 °C, and the concentration of DCPM aqueous dispersions varied from 0.5 to 2 wt%. The results are shown in Fig. 14.

As presented in Fig. 14. The viscosity increases with an increase of DCPM, and the changing law is consistent with the variation trends of viscosity versus concentration of liner polymer. This is because the more concentration of DCPM, the more formation of liner polymer. Moreover, the polymer chains tangle with each other and thus increases the viscosity.

3.6.3 Degradable performance of DCPM in oil dispersions

The viscosity of DCPM oil dispersions remained unchanged (about 10 mPa·s, it is the same value as the viscosity of oil) regardless of the DCPM content(Fig. 15, see in

supplementary information) and aging temperature.(Fig.16, see in supplementary information) In addition, it was observed that amounts of particle aggregates attached to the bottom/wall of the testing bottle. These appearances indicated that DCPM couldn't thicken the oil, which indirectly demonstrated that DCPM should not cause damage to the oil layer when injected to the formation.

3.7 Sandpack flooding experiments

3.7.1 One dimension sandpack flooding experiments

One dimension sandpack flooding experiments were conducted to discover the injectivity and enhanced oil recovery effectiveness of DCPM, the results are shown in Fig. 17 and Table 6.

In Fig.17, the injected pressure kept constant in the first water flooding stage, which indicated the injecting water channeled through the water-thief zone and large amounts of unrecovered hydrocarbon were remained, thus resulting in poor recovery of 10.9%(Table 6). Subsequently, the pressure sharply increased and then fluctuated with the flooding of DCPM. The reasons are listed as follows. When DCPM plugged the pore-throats, the pressure climbed to the maximum value, and then DCPM distorted after absorbing water and successfully passed through the pore throat under the driving of injecting water, which led to the dropped pressure. Afterwards, the pressure continued to rise when the next plugging was achieved, this process was reduplicated again and again, which resulted in the fluctuating pressure. At the secondary water flooding stage, the pressure initially increased, which was due to the highly viscous polymer solution formed by the degradation of DCPM. After that, the dilution effect to polymer by subsequent injecting water resulted in the dropping pressure. However, the final pressure was stable and higher than that of the first water flooding, which demonstrated that the polymer flooding within deep formation occurred to enhanced oil recovery. In addition, the recovery of 31.7% resulted from DCPM flooding and secondary water flooding manifested that DCPM could improve the heterogeneity of inner layer and enhanced oil recovery effectively.

3.7.2 Parallel sandpicks flooding experiments

Parallel sandpicks flooding experiments were prepared to test the profile control performance and enhanced oil recovery performance of DCPM.

As listed in Table 7. After first water flooding, the oil recovery in 2# sandpack (high

permeability) is higher than that of in 3# sandpack(low permeability), which indicates that amounts of un-swept oil remains in low permeability. However, after DCPM flooding and secondary water flooding, the oil recovery are improved in both sandpacks, but 3# sandpack exhibits higher oil recovery compared with 2# sandpack. What's more, the permeability of both sandpacks are basically the same after control. Which demonstrates that DCPM can improve the interlayer heterogeneity by plugging high permeability, and diverts the subsequent water into the low permeability layer to enhance the oil recovery.

4. Conclusions

In this work, DCPM with diameter of 5~10 microns was synthesized by inverse emulsion polymerization. FT-IR, ¹H-NMR and elemental analysis confirmed that DCPM contained the structure of AM,AMPS,HM and PEG-200 diacrylate. The degradation performance of DCPM was carried out by SEM and viscosity experiments, which demonstrated that the degradation process of DCPM was from initially swelling to breaking down into linear polymer. Furthermore, sandpacks flooding experiments indicated that DCPM could correct reservoir heterogeneity and improve conformance control, which could be used as conformance control agent. Meanwhile, DCPM could achieve polymer flooding within deep formation after it degraded into a highly viscous polymer solution to improve oil recovery.

In conclusion, DCPM is recommended for deep conformance control and oil displacement in enhanced oil recovery applications.

Reference

1. B. Bai, L. Li, Y. Liu, H. Liu, Z. Wang and C.You, *SPE Reserv. Eval. Eng.*,2007, **10**, 415.
2. Y. Liu, M. Zhu, X. Liu, W. Zhang, B. Sun, Y. Chen and P.A. Hans, *Polymer.*, 2006,**47**, 1.
3. R.D. Sydansk and G.P. Southwell , *SPE Prod. Facil.*, 2000,**15**,270.
4. R.S. Seright, R.H. Lane and R.D. Sydansk, *SPE Prod. Facil.*,2003, **18**, 158.
5. M. Salehi, at the 18th *SPE Symposium on Improved Oil Recovery*, USA, April, 2012.

6. J. Li, Y. Liu, N. Zhang, Zh. Zeng and H. Jiang, *J. Disper. Sci. Technol.*, 2014,**35**,120.
7. Ch.Yao, G. Lei, X.Gao and L.Li, *J. Appl. Polym. Sci.*, 2013, **130**,1124.
8. G.Lei , L. Li and A. Hisham, *SPE Reserv. Eval. Eng.*,2011,**2**,120.
9. Ch.Yao, G. Lei, M. Lawrence and S.Tammo, *Environ. Sci. Technol.*,2014, **48**, 5329.
10. H.Frampton, at the 14th *SPE Symposium on Improved Oil Recovery*, Tulsa, April, 2004.
11. J.Pritchett , at the *SPE International Improved Oil Recovery Conference in Asia Pacific*, Kuala Lumpur, October,2003.
12. D.Rousseau , at the *SPE International Symposium on Oilfield Chemistry*, Texas, February,2005.
13. A.Mazen, H. Chun, S. Kamy and D. Mojdeh, *J.Petrol.Sci.Eng.*, 2014,**122**,741.
14. T. Paul and B. Bai, *J.Petrol.Sci.Eng.*, 2014, **124**,35.
15. Zh.Ye, G.Gou, Sh. Gou, W. Jiang and T. Liu, *J.Appl.Polym.Sci.*, 2013,**128**, 2003.
16. P. S.Mohanty, H. Dietsch, L. Rubatat, A. Stradner, K. Matsumoto, H. Matsuoka and P.Schurtenberger, *Langmuir.*, 2009,**25**, 1940.
17. C.Kevin and A.Taylor, *J.Petrol.Sci.Eng.*, 1998, **19**, 265.
18. C.A.Grattoni, H.H.Al-Sharji, C.Yang, A.H.Muggeridge and R.W. Zimmerman, *J.Colloid. Interf.Sci.*, 2001,**240**,601.
19. J.W. Vanderhoff, E. B. Bradford, M. L. Tarkowski, J. B. Schaffer and R. M. Wiley, *Ad. Chem. Ser.*, 1962,**34**, 32.
20. R. A. Siegel and B.A. Firestone, *Macromolecules.*,1988,**21**, 3254.
21. T. G. Park and A. S. Hoffman, *J. Appl. Polym. Sci.*,1992, **46**, 659.
22. K. Suda and P. Pattama, *J.Appl.Polym.Sci.*,1999,**72**, 1349.
23. S. Peng and C. Wu, *Macromolecules.*, 1999,**32**,585.

Captions

Fig. 1 Schematic of DCPM for deep profile control and oil placement in heterogeneous reservoirs

Fig. 2 IR spectrum of PAM and DCPM

Fig.3 ¹H-NMR analysis of DCPM

Fig. 4 Particle size analysis of DCPM

Fig. 5 Mechanical stability of DCPM

Fig. 6 Effect of monomer concentration on particle size and conversion rate

Fig. 7 Effect of monomer ratio on particle size and conversion rate

Fig. 8 Effect of the volume ratio of oil to water on particle size and conversion rate

Fig. 9 Effect of the emulsifier concentration on particle size and conversion rate

Fig. 10 SEM of decomposition process of DCPM

Fig. 11 Effect of salinity on decomposition of DCPM

Fig. 12 Effect of temperature on decomposition of DCPM

Fig. 13 Effect of PEG-200 diacrylate concentration on decomposition of DCPM

Fig. 14 Effect of DCPM content on decomposition of DCPM

Fig. 15 Effect of DCPM content on decomposition of DCPM in oil phase

Fig. 16 Effect of temperature on decomposition of DCPM in oil phase

Fig. 17 The variation curve of injected pressure at different stage

Table 1 Basic parameters of sandpacks

Table 2 Molar composition of DCPM

Table 3 Recipe of DCPM

Table 4 The effect of initiator on the polymerization

Table 5 Viscosity of DCPM at different aging days

Table 6 Oil displacement effect of one dimension sandpack flooding

Table 7 Oil displacement effect of parallel sandpacks flooding

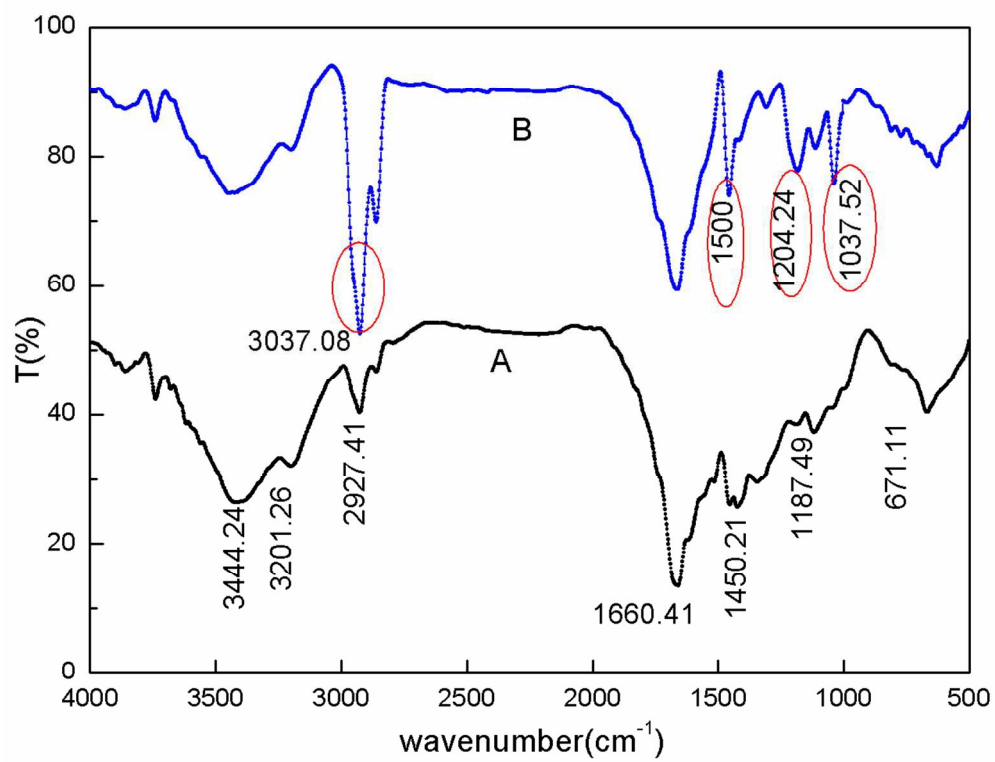


Fig. 2 IR spectrum of PAM and DCPM
217x167mm (150 x 150 DPI)

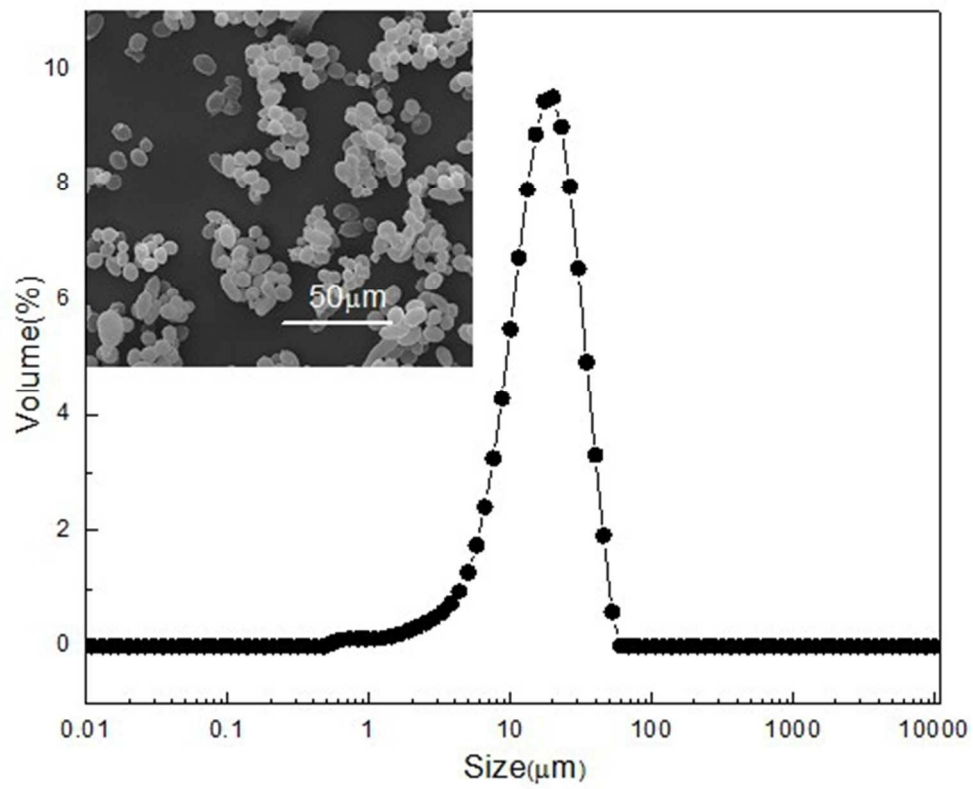


Fig. 4 Particle size analysis of DCPM
138x112mm (96 x 96 DPI)

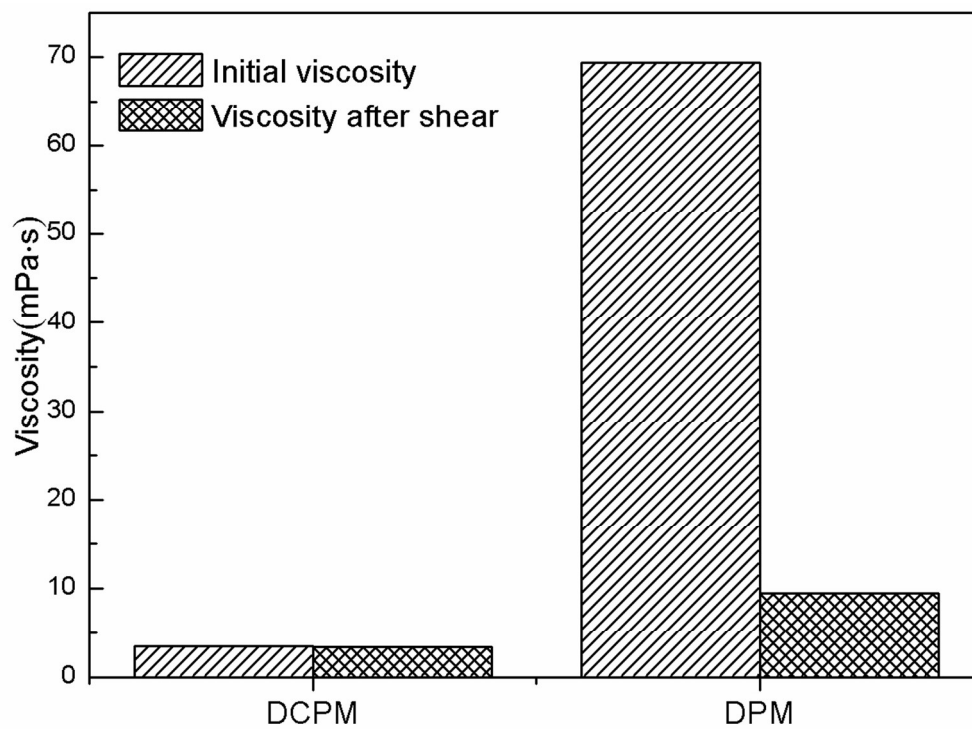


Fig. 5 Mechanical stability of DCPM
213x156mm (150 x 150 DPI)

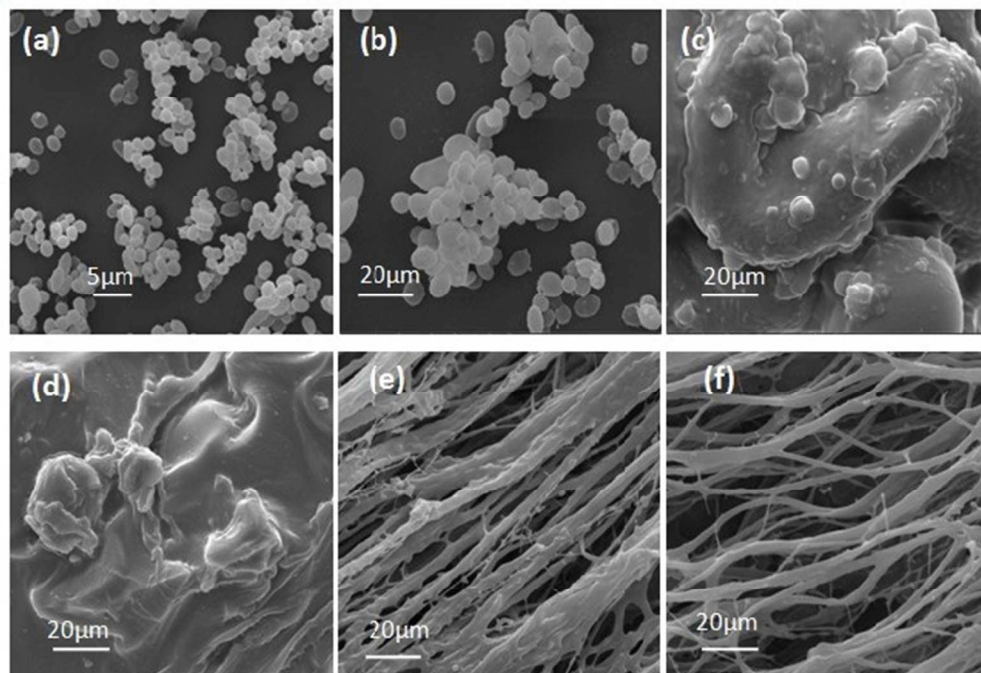


Fig. 10 SEM of decomposition process of DCPM
171x118mm (96 x 96 DPI)

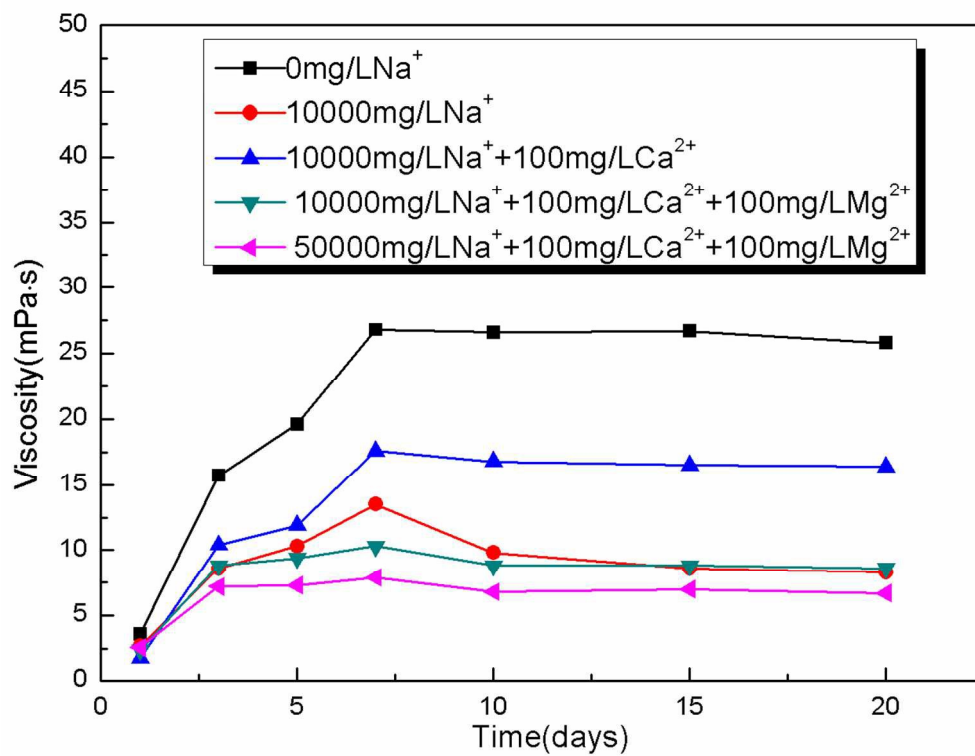


Fig.11 Effect of salinity on decomposition of DCPM
216x165mm (150 x 150 DPI)

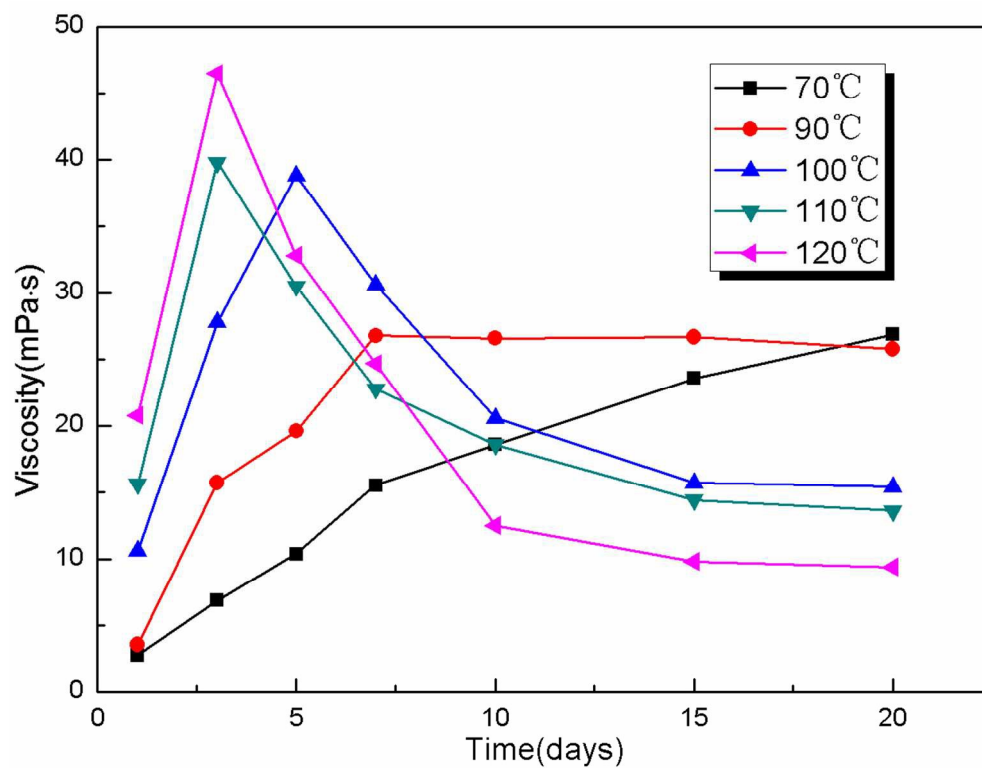


Fig. 12 Effect of temperature on decomposition of DCPM
213x164mm (150 x 150 DPI)

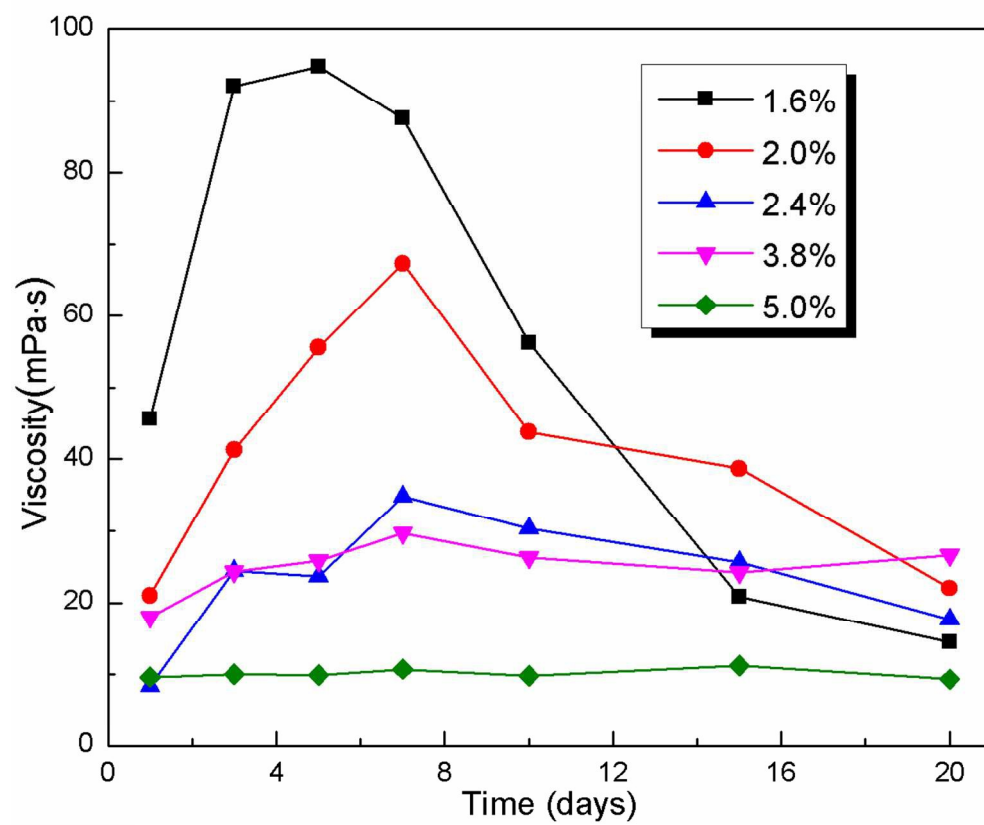


Fig. 13 Effect of PEG-200 diacrylate concentration on decomposition of DCPM
216x179mm (150 x 150 DPI)

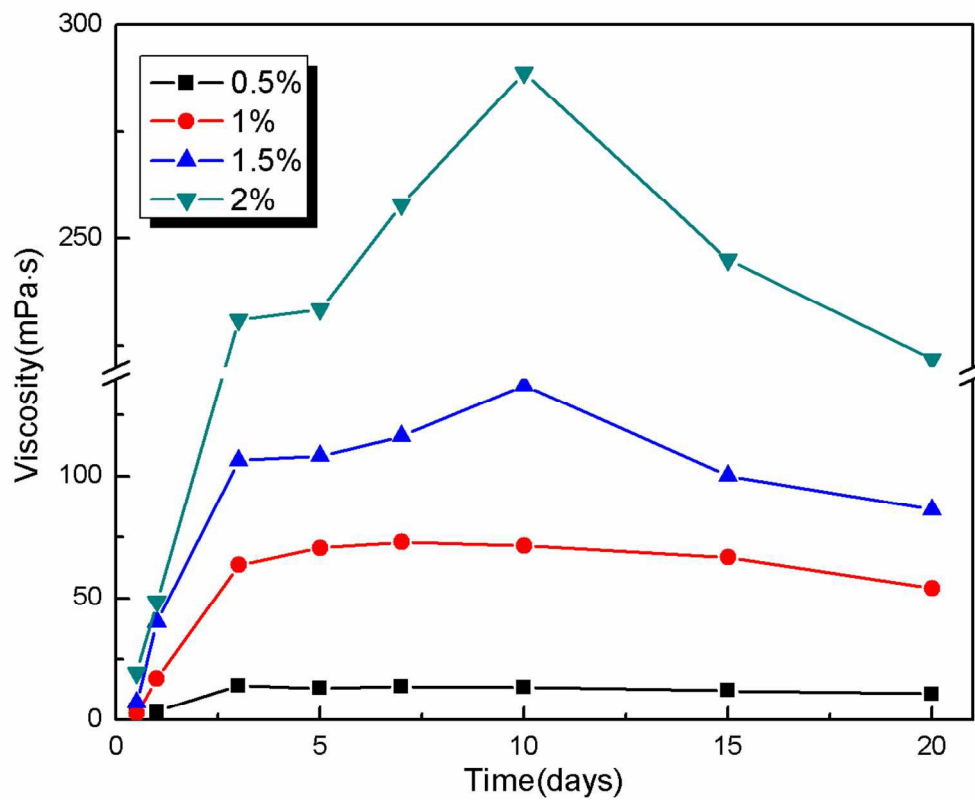


Fig. 14 Effect of DCPM content on decomposition of DCPM
222x180mm (150 x 150 DPI)

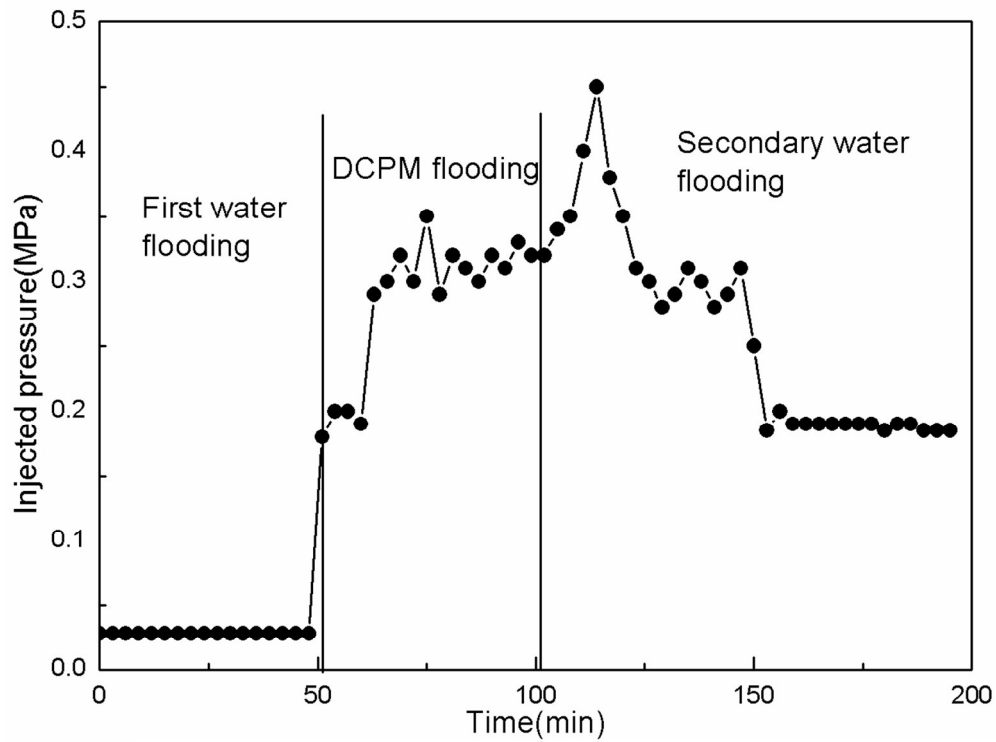


Fig. 17 The variation curve of injected pressure at different stage
218x163mm (150 x 150 DPI)

Table 2 Molar composition of DCPM

Samples	Molar composition of DCPM/ mol%			
	AM	AMPS	HM	PEG-200 diacrylate
Monomer feed composition	90.72	8.81	0.55	0.41
DCPM composition	88.59	9.19	0.46	0.31

Table 5 Viscosity of DCPM at different aging days

Aging time/day	1	3	5	7	10	15	20
Viscosity/mPa·s	3.6	15.4	18.9	25.6	26.8	26.4	26.6

Table 6 Oil displacement effect of one dimension sandpack flooding

Code	Gross recovery/%		
	First water flooding	DCPM flooding	Secondary water flooding
1#	10.9	18.4	42.6

Table 7 Oil displacement effect of parallel sandpacks flooding

Code	Gross recovery/%			Permeability/ $\times 10^{-3} \mu\text{m}^2$		Plugging rate/%
	First water flooding	DCPM flooding	Secondary water flooding	Before control	After control	
2#	44.5	50.7	57.2	2532.4	208.9	91.7
3#	8.6	11.8	32.4	925.3	175.6	81.0